

# Adaptive Imaging Spectrometer in a Time-Domain Filtering Architecture

Yang Jiao, Sameer R. Bhalotra, Helen L. Kung, and D. A. B. Miller

*Edward L. Ginzton Laboratory*

*Stanford University, Stanford, CA 94305-4085*

Collecting a spectrum for each pixel in an image can give much useful information about a scene, such as chemical content, but generates a vast amount of data. Optical filters can select specific spectral features in advance, but are difficult to adapt in real time to different desired spectra. We have constructed an imaging spectrometer using a time-domain filtering architecture, capable of real-time spectral feature extraction and adaptation to different desired spectra. We demonstrate in real-time the abilities both to (i) recognize multiple specific colors in an image, and (ii) recognize individual colors while suppressing combinations of the same colors, an example of a sophisticated signal processing function that can be performed in this architecture.

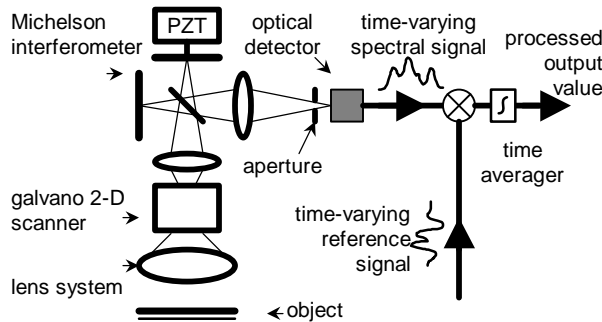


Figure 1. Time-domain filtering setup

The architecture is illustrated in Fig. 1. One pixel of an image is interfered with itself on an optical detector at the exit of a Michelson interferometer. Scanning one interferometer arm generates a time-varying spectral signal, which is multiplied by a time-varying reference signal, and the result is integrated to give the output. Only one single data value per pixel per time-domain filter is generated instead of an entire sampled interferogram per pixel as in a conventional Fourier transform (FT) imaging spectrometer (FTS). For a small number of filters, this presents a significant reduction in the amount of data to be transmitted, stored, and processed. This architecture is applicable to many low to medium spectral resolution detection applications, including certain types of remote sensing and medical diagnosis applications<sup>1,2</sup>. The time-domain filtering architecture eliminates the need for Fourier transforms and compensation for mirror scan nonlinearities<sup>3</sup>. Instead of performing a FT on the interferogram as in a conventional FTS, the overlap integral of the interferogram and a predetermined reference function is carried out in real-time during data collection, either to indicate the presence or absence of

a spectral signature or to perform certain types of signal processing. This allows for switching on demand between various signal processing and spectral signature extraction configurations by changing the reference functions. No mechanical or data path reconfiguration is used. This system allows very simple spectrometers to perform sophisticated sensing tasks with minimal data processing power.

One way to obtain a reference function for spectral signature detection is to record the interferogram from a source with the desired spectral signature. This automatically takes care of any nonlinearities in the mirror scan rate, in contrast to a conventional FTS which requires an exactly linear scan in time. For example, Fig. 2(a) shows a nonlinear scan interferogram for a yellow LED source serving as the yellow reference function for this experiment. An example of signal processing that can be incorporated into the reference function is the simultaneous suppression of a two-component spectral signature and detection of the two components if they occur separately. Let  $R(t)$  and  $G(t)$  be the reference functions of the two components. The inhibitory reference function  $I(t)$  is given by:

$$I(t) = R(t) - bG(t), \quad (1)$$

where  $b$  is the ratio between the intensities of the two components. Fig. 2(b) shows an inhibitory reference function for a red and green two-color LED source.

The experimental setup is shown in Fig. 1. A lens system collects the light from the object. The light then passes through a 2-D raster scan galvano mirror set, which determines which pixel is sent through a Michelson interferometer. A piezo-electric transducer (PZT) actuator varies the path length of one interferometer arm. The interferogram for each pixel is collected by an amplified silicon photodetector. The PZT actuation, raster scanning, and data acquisition are controlled and synchronized through a PC.

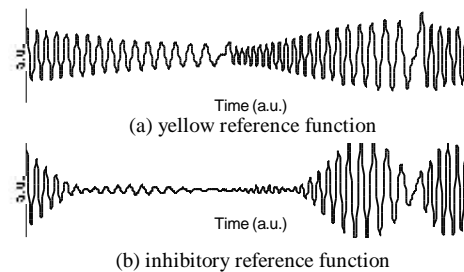


Figure 2. Reference functions

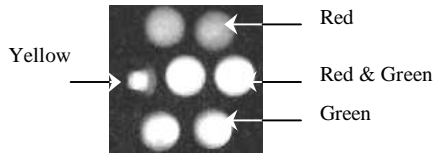


Figure 3. Conventional camera intensity image of object. All LEDs have diffused covers except the yellow, which appears smaller.

To demonstrate the robustness of the discrimination system, the PZT is driven by a 30 Hz DC-offset sinusoid rather than the linear scan required by a conventional FTS. The PZT scan length is set to 13  $\mu\text{m}$  in this experiment, and determines the spectral resolution of the imager. To average the detector pre-amplifier noise, the interferogram is recorded for 3 periods of the PZT scan for each pixel. The photodetector has a diameter of 0.9mm, and an aperture of 0.5mm is placed before the photodetector to increase the spatial resolution. After amplification and noise filtering by a band pass filter, the raw interferogram is sent to the controller PC. For this demonstration, the PC calculates the overlap integrals between the interferogram and the recorded reference functions, though we believe the task can also be performed by simple analog circuitry.

In this experiment, four reference functions are generated. Three of them are single spectrum signature reference functions generated by the average of 32 recorded interferograms by the system (e.g., Fig. 2(b)). The fourth inhibitory reference function suppresses the output when a particular ratio of red and green spectral signatures are present, but will generate a signal when only one of the spectral signatures is present. The inhibitory reference is a weighted difference of the red and green references. Expansion to more than four reference functions is trivial, requiring only the incorporation of additional multiplication and integration channels in either software or hardware.

Fig. 3 shows the object imaged by a conventional camera with annotation of the LED colors. The two-color "Red & Green" LEDs in the middle row simultaneously emit both red and green light. Figures 4 (a,b,c) show the output of the imaging spectrometer after applying the single spectral signature reference functions. Even though the ratio of the red and green intensities in the two-color LEDs are adjusted so that their visually perceived color is indistinguishable from the true yellow LED, the two-color LEDs correctly appear in both green and red channels but not the yellow channel. The system completely separated the red and green spectral signatures in Fig. 4 (a,b), distinguishing also between the true yellow and the apparent yellow of the red-green mixture. The yellow and green spectral peaks are separated by 30 nm, which is in the spectral resolution limit obtainable from a 13

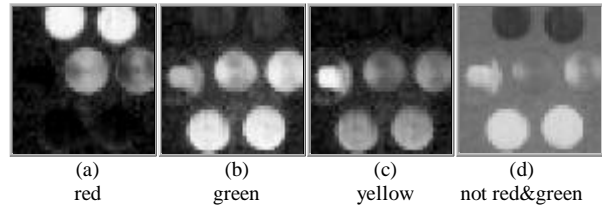


Figure 4. 40X40 pixel images generated by the overlap integral with four reference functions. In a), b) and c), bright areas indicate the presence of a spectral signature. In d), points that only contain a green component are represented by bright pixels; red is represented by dark pixels, points that contain either both of the spectral signatures or none of the spectral signature are represented by gray.

$\mu\text{m}$  interferogram, and leads to only partial discrimination between green and yellow spectral signatures. The result of applying the inhibitory reference function (Fig. 2(b)) is shown in Fig. 4(d). The signals from the two-color LEDs are suppressed where the red and green signatures mixed finer than the imaged pixel size. The resulting image has drastically enhanced contrast between the two-color LEDs and the single color LEDs. The perimeters of the two-color LEDs, the right most one in particular, contain more of the green spectral signature. This detail can be visually confirmed and correctly appears in Fig. 4(d), in which the perimeters of the two-color LEDs are lighter.

These results demonstrate the successful operation of an adaptive time-domain filtering multispectral imaging system. The time-domain filtering architecture allowed for rapid reconfiguration to perform various spectral feature extraction and signal processing tasks, including tasks beyond those of a simple color camera. Inherent minimal data transmission, storage, and post processing considerably eased requirements on the imager hardware design. These advantages of the time-domain filtering architecture, along with its tolerance to scan non-linearities, will aid the design and expand the applications of inexpensive, mobile hyperspectral and multispectral imaging systems.

This material is based upon work supported by the United States Air Force under contract No. F49620-00-C-0040. Support was provided by a DARPA grant for Photonic Wavelength And Spatial Signal Processing, under a sub contract from FMA&H. YJ acknowledges the support of the NSFGRF and the Reed-Hodgson SGF. SRB gratefully acknowledges the support of the Regina Casper Stanford Graduate Fellowship. HLK was supported by Lucent Technologies GRPW grant.

<sup>1</sup> R.J. McNichols, G.L. Coté, "Optical glucose sensing in biological fluids," *Journal of Biomedical Optics* 5(1), 5 (2000).

<sup>2</sup> N. Gupta, R. Dahmani, "Multispectral and Hyperspectral Imaging with AOTF for Object Recognition," *Proc. SPIE* 3584, 128 (1999).

<sup>3</sup> S. R. Bhalotra, H. L. Kung, and D. A. B. Miller, "Real-time discrimination of spectra by time-domain adaptive filtering in a Fourier transform interferometer," in *Conference on Fourier Transform Spectroscopy 2001*, Coeur d'Alene, ID (Feb 5-8, 2001). Paper PDP2.